Case Studies in Thermal Engineering 6 (2015) 104–115

Contents lists available at ScienceDirect

Case Studies in Thermal Engineering

journal homepage: www.elsevier.com/locate/csite

Heat transfer of swirling impinging jets ejected from Nozzles with twisted tapes utilizing CFD technique

Younes Amini [a,*], Mojtaba Mokhtari [b], Masoud Haghshenasfard [a], M. Barzegar Gerdroodbary [c]

[a] Department of Chemical Engineering, Isfahan University of Technology, Isfahan, Iran
[b] Department of Chemical and Petroleum Engineering, Sharif University of Technology, Tehran, Iran
[c] Department of Mechanical Engineering, Babol Noshirvani University of Technology, Babol, Iran

ARTICLE INFO

Article history:
Received 12 June 2015
Received in revised form
2 August 2015
Accepted 11 August 2015
Available online 12 August 2015

Keywords:
Swirling impinging jets
Twisted tapes
CFD
Nusselt number
Heat transfer

ABSTRACT

This research investigated the forced convection heat transfer by using the swirling impinging jets. This study focused on nozzles, which equipped with twisted tapes via a numerical approach. The computational domain created by utilizing the fully structured meshes, which had very high quality from the viewpoint of aspect ratio and skewness. The numerical simulations were performed at four different jet-to-plate distances (L/D) of 2, 4, 6 and 8, four Reynolds numbers of 4000, 8000, 12,000 and 16,000, and also four different twist ratios (y/w) of 3, 4, 5 and 6. The mesh-independent tests were conducted based upon the average Nusselt number. The obtained results revealed good agreement with the available experimental data from the open literature. It was observed that for jet-to-plate distances of $L/D=6$ and $L/D=8$, the heat transfer rate of swirling jets was more than regular jets, and heat transfer rate at higher Reynolds numbers increased due to the greater rate of momentum transfer. Besides, the calculation done for a pair of jets, and the results shown that using two jets, instead of one, could increase the rate of heat transfer in the same air flow rate.

1. Introduction

Implementation of swirling impinging jets is an important method for increasing the heat transfer rates and could be used for various drying and cooling systems. The results obtained from different studies have showed that using of swirling impinging jets in different fields such as food industries, cooling of turbine blades, and electronic equipment leads to an increase in the heat transfer rates and further economic savings. The reason why swirling impinging jets are in such a great demand is that they induce high heat transfer rates specifically in the stagnation zone. Many studies such as the study performed by Goldstein and Behbahani [1] showed that the Nusselt number is maximum at the stagnation zone and has low values in other areas. One way to avoid this occurrence is using swirling jet instead of normal jet. The fluid flow in swirling jets is quite well known and is closely associated with the nozzle diameter as well as the distance between the nozzle and the plate [2,3]. This flow might be divided into several distinct regions: the entrance zone, the

* Corresponding author.
E-mail address: y.amini@ce.iut.ac.ir (Y. Amini).

http://dx.doi.org/10.1016/j.csite.2015.08.001
2214-157X/

Nomenclature

A	Heat transfer area, [m^2]
C_p	Specific heat capacity, [$kJ\,kg^{-1}\,K^{-1}$]
C_1, C_2, C_μ	Constant of the k–ε model, [–]
D	Diameter of Nozzle, [m]
D_h	Hydraulic diameter, [m]
E	Total energy, [J]
E_{ij}	Linear deformation rate, [s^{-1}]
g	Gravitational acceleration, [$m\,s^{-2}$]
h	Heat transfer coefficient, [$W\,m^{-2}\,K^{-1}$]
K	Thermal conductivity, [$W\,m^{-1}\,K^{-1}$]
L	Nozzle-to-surface spacing, [m]
Nu	Nusselt number, [–]
P	Static pressure, [Pa]
Q	Heat transfer rate, [W]
r	Distance from center of the surface, [m]
Re	Reynolds number, [–]
T	Temperature, [K]
u, u_i, u_j	Mean velocity components, [ms^{-1}]
x_i, x_j	Cartesian coordinates, [m]
Y	Length of one turn of tape, [m]
W	Tape width, [m]

Greek symbols

ε	Dissipation rate, [$W\,kg^{-1}$]
K	Turbulent kinetic energy, [$J\,kg^{-1}$]
μ, μ_T, μ_{eff}	Laminar, turbulent and effective viscosity, [Pa s]
V	Kinematic viscosity, [m^2/s]
ρ	Density, [$kg\,m^{-3}$]
σ_K, σ_ε	Turbulent Prandtl numbers for K–ε, [–]

swirling jet zone, and the flow separation zone [4]. In order to develop the application of this method, extensive efforts have been made. Saha [5] experimentally studied the heat transfer and the pressure drop air turbulent flow through rectangular ducts with combined internal axial corrugations and with twisted tape inserts with and without oblique teeth. The results showed that axial corrugations and oblique teeth increased the *Nusselt number.* Nanan et al. [6] did *an* experimental study on the forced convective heat transfer on a plate cooled by swirling impinging jets. Their results showed that the maximum Nusselt number was occurring when the twist ratio and Reynolds Number were high and jet-to-plate distance was low. Katti and Prabhu [7] performed an experimental investigation to determine the effect of jet-to-plate spacing and Reynolds number on the local heat transfer. They reported that the increase in Reynolds number increases the heat transfer at all the radial locations and the Nusselt number at stagnation point increases with increasing the jet-to-plate distance. Tummers et al. [8] investigated turbulent flow in the stagnation point of a swirling impinging jet around a pipe, and calculated the average fluid velocity and the Reynolds stresses. Eiamsa-ard et al. [9–11] experimentally and numerically studied the influence of helical tapes placed in a tube on forced convective heat transfer. Their results showed that using the helical tapes might increase the rate of heat transfer up to 50%. Ndao et al. [12] conducted an experimental study on heat transfer during impingement of swirling jets on a small surface with metal fins. They concluded that as a result of using swirling impinging jets, the heat transfer coefficient was increased by 200%. Sagot et al. [13] studied the heat transfer effects of a symmetrical swirling jet passing against a grooved surface under constant wall temperature conditions. The grooves had a square or triangular cross sections with depth and pitch of 1 mm and 2 mm, respectively. Under such circumstances, the rate of heat transfer increased by 81% as compared to the flat plate. Rahimi et al. [14] investigated the experimental and numerical studies on heat transfer of a tube equipped with twisted tape. They used some modified twisted tapes and studied on their effects on the heat transfer rate. Kanokjaruvijit and Martinez-Botas [15] investigated the heat transfer induced by a group of impinging jets on the semi spherical concave surface impressions with a checkered arrangement. The impressions in the surface increased the heat transfer rate by about 70% as compared to a flat surface. Using low-depth hollows with large radii of curvature effectively increased the rate of heat transfer. Gulati et al. [16] did an experimental study on the influence of the shape of the nozzle on local heat transfer in impinging jets. Their results revealed that Nusselt numbers are insensitive to the shape of the nozzle.

Salman et al. [17] investigated the experimental and computational fluid dynamics (CFD) modeling to studies the effect of the swirl intensity on the heat transfer characteristics of conventional and swirl impingement air jets at a constant nozzle-to-plate distance ($L=2D$).

Wannassi and Monnoyer [18] used the flow and heat transfer characteristics of a staggered combination of straight and swirling jets in order to access flow details and to show complex flow structures as well as the strong coupling between the feeding and the exhaust phases experienced by the cooling air.

The effect of jet geometry on the flow and the heat transfer characteristics was investigated experimentally and numerically for elliptic and rectangular impinging jet arrays by Caliskan et al. [19].

Recently, San and Chen [20], studied the effect of cross flow, jet interaction and jet interference on heat transfer distribution for five confined circular air jets impinging on a flat plate. They noticed that the s=D appears to be the major factor affecting the non-uniformity of heat transfer, while the H=D is a minor factor.

In the recent numerical study of Saqr and Wahid [21], a Rankine type vortex structure was added to the flow to create a swirl and the intensity of swirl is related to the ratio between axial thrust of tangential momentum and the axial thrust of axial momentum.

Computational fluid dynamics, as a research tool, can complete the results of experimental studies by calculating the desired parameters at regions or situations in which experimental work is expensive or impossible [22–27].

In the present work, the CFD code was utilized to obtain numerical solutions of swirling impinging jets which ejected from nozzles that equipped with twisted tapes. The effects of jet-to-plate distance, as well as the different Reynolds numbers investigated for four various twist ratios. The conditions for the same twist ratios and jet-to-plate distances then investigated at four different Reynolds numbers. Besides, numerical solution was done in two-jet cases, and results shown that using two jets instead of one, increased the rate of heat transfer, although the air flow rate was equal, so the cooling efficiency would be increased by using two jets.

The main contribution of this study is the investigation of swirling impinging jet on the heat transfer of the hot plate to clarify the role of swirling flow and performance of this device on cooling. Furthermore, the efficiency of two swirling jet on heat flux of flat plate was studied. Moreover, the complicated flow structure of two jets interaction on the plate is revealed.

In the numerical method presented in this research, an effort was made to closely adapt the conditions of simulation to those of the actual experimental setup of Nanan et al. [6]. In their study, inserted inside the nozzle was a metal tape, twisted in three-dimensions to induce swirling in the fluid flow. This twisted tape transformed the simple one dimensional nozzle flow into a complicated three-dimensional one.

2. Governing equations

In the current study, the CFD code was used for three-dimensional numerical simulations of fluid flow and heat transfer. The developed model simultaneously solves the mass, momentum, and energy conservation equations. Generally, for an incompressible flow, these equations are as follows:

$$\frac{\partial \rho}{\partial t} + \nabla.\,(\rho \bar{u}) = 0 \tag{1}$$

$$\frac{\partial(\rho \bar{u})}{\partial t} + \nabla.\,(\rho \bar{u}\ \bar{u}) = \rho g - \nabla P + \nabla.\,\bar{\bar{\tau}} \tag{2}$$

$$\frac{\partial(\rho e)}{\partial t} + \nabla.\,(\bar{u}(\rho e + P)) = \nabla\big(K_{eff}\nabla T + \nabla.\,(\bar{\bar{\tau}}_{eff}\bar{u})\big) \tag{3}$$

In which,

$$\bar{\bar{\tau}} = \mu(\nabla\bar{u} + \nabla\bar{u}^{T} - \frac{2}{3}\nabla\bar{u}I) \tag{4}$$

Due to the random behavior of the turbulent flow, the calculations could not be based on a single comprehensive description for motion of all fluid elements. The turbulent flow is described through velocity variations. These variations carry small amounts of energy and momentum at high frequencies in a small scale. Therefore, turbulent flow should be modeled directly in the calculations. In this regard, the κ–ε turbulence equations of the renormalization group (RNG) type with near-wall functions to predict the flow behavior near the wall, as well as the governing rotational flow equations was implemented. The equations utilized were obtained from Rahimi et al. [14] and are given as:

$$\mu_{eff} = \mu + \mu_t, \quad \mu_\tau = \rho C_\mu \frac{\kappa^2}{\varepsilon} \tag{5}$$

$$\frac{\partial(\rho\kappa)}{\partial t} + \frac{\partial}{\partial x_i}(\rho\kappa u_i) = \frac{\partial}{\partial x_i}\left(\frac{\mu_{eff}}{\sigma\kappa}\frac{\partial\kappa}{\partial x_i}\right) + \mu_t\frac{\partial}{\partial x_i}\left(\frac{\partial u_i}{\partial x_i} + \frac{\partial u_j}{\partial x_j}\right)\frac{\partial u_i}{\partial x_j} + \rho\varepsilon \tag{6}$$

$$\frac{\partial(\rho\varepsilon)}{\partial t} + \frac{\partial}{\partial x_i}(\rho\varepsilon u_i) = \frac{\partial}{\partial x_i}\left(\frac{\mu_{eff}}{\sigma_\varepsilon}\frac{\partial\varepsilon}{\partial x_i}\right) + C_{1\varepsilon}\frac{\varepsilon}{\kappa}\mu_t\left(\frac{\partial u_i}{\partial x_i} + \frac{\partial u_j}{\partial x_j}\right)\frac{\partial u_i}{\partial x_j} + - C_{2\varepsilon}\rho\frac{\varepsilon^2}{\kappa} - \alpha\rho\frac{\varepsilon^2}{\kappa} \tag{7}$$

where,

$$\alpha = C_\mu \eta^3 \frac{\left(1 - \frac{\eta}{\eta_0}\right)}{1 + \beta\eta^3}, \quad \eta = E\frac{K}{\varepsilon}, \quad E2 = 2E_{ij}E_{ij}, \quad E_{ij} = 0.5\left(\frac{\partial u_i}{\partial x_i} + \frac{\partial u_j}{\partial x_j}\right) \tag{8}$$

In the present study, the heat transfer coefficient, h, the Nusselt number, Nu, and the Reynolds Number, Re, are estimated as follows:

$$h = \frac{(q_{\text{surface}})}{T_{\text{surface}} - T_{\text{bulk}}}$$

$$\text{Nu} = \frac{hD}{K}$$

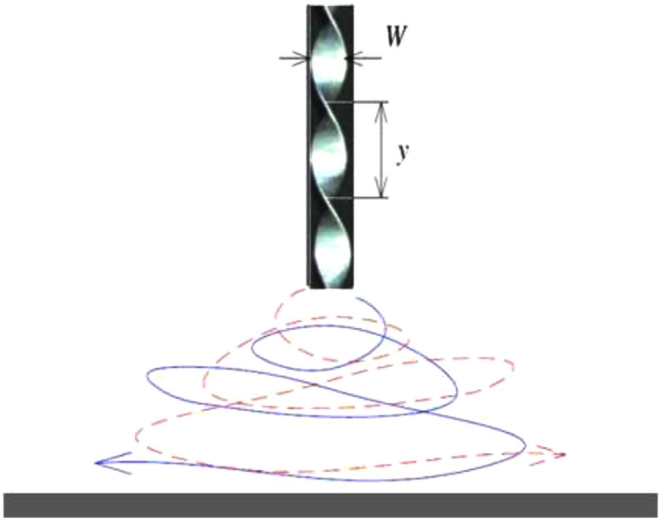

Fig. 1. Geometry of computational domain [4].

$$\mathrm{Re} = \frac{\rho u D}{\mu}$$

3. Numerical simulation

To obtain numerical solutions, a suitable high quality computational domain with sufficient number of elements created. The geometry and generated mesh were shown in Figs. 1 and 2. It should be emphasized that the total number of elements were limited due to limitations imposed by the existing hardware (core i7 CPU 3.4 GHz, 8 GB RAM). For generating the mesh, three-dimensional structured elements were utilized due to their efficiently in handling complicated geometries and turbulent flow situations, as well as producing minimum errors. As a first guess, elements with average side lengths of 0.8, 0.6, 0.5 and 0.4 mm were used to establish the computational domain. Upon solving the flow field and the energy equations, the corresponding Nusselt numbers were computed. The details results obtained from these calculations are given in Table 1. As can be observed, the relative errors in the calculation of the Nusselt number for the 0.4 and 0.5 mm elements were less than 1%. Therefore, the mesh with mean dimensions of 0.5 mm was selected as the threshold of the computational domain in order to apply the numerical simulation.

To ensure the mesh quality, the histogram for the parameters aspect ratio and skewness were plotted. As the aspect ratio of most elements did not exceed 3 and skewness was also within the very reasonable range of less than 0.5, it was concluded that the mesh quality was fully acceptable.

The finite volume method was used for the numerical solutions. The SIMPLE algorithm was selected for computing the pressure–velocity coupling and the first order upwind discretization for momentum, energy and turbulent kinetic energy was utilized. The convergence criterion of the residual errors was set to 10^{-8}. In Fig. 3, the obtained values are compared with the corresponding experimental values reported by Nanan et al. [6]. As observed, the comparison is performed at two different jet-to-plate distances of $L/D=2$ and 4 with the Reynolds numbers set to 8000 and 12,000, respectively.

Note that the Nusselt number was calculated at the centerline of the impinged plate. As observed, the results are in good agreement with those in the previously published literature. Hence, the accuracy and stability of the method used for the numerical computations were verified.

Table 2 shows the information of all cases which are studied in the present work.

4. Results and discussion

After the validation of the present model, several numerical solutions were executed so that the effect of different swirling jet parameters on the effective heat transfer rate could be investigated. The significant parameters in a swirling jet are the jet-to-plate distance (L/D), the Reynolds number and the twist ratio (y/w).

Fig. 4 shows typical velocity contours between the ejected jet and the impinged plate for $L/D=6$ under different Reynolds numbers. As is obvious in this figure, increase in the jet Reynolds number can increase the amount of velocity near the hot surface, which can lead to a bigger Nusselt number. Although using twisted tape can decrease the Nusselt Number of

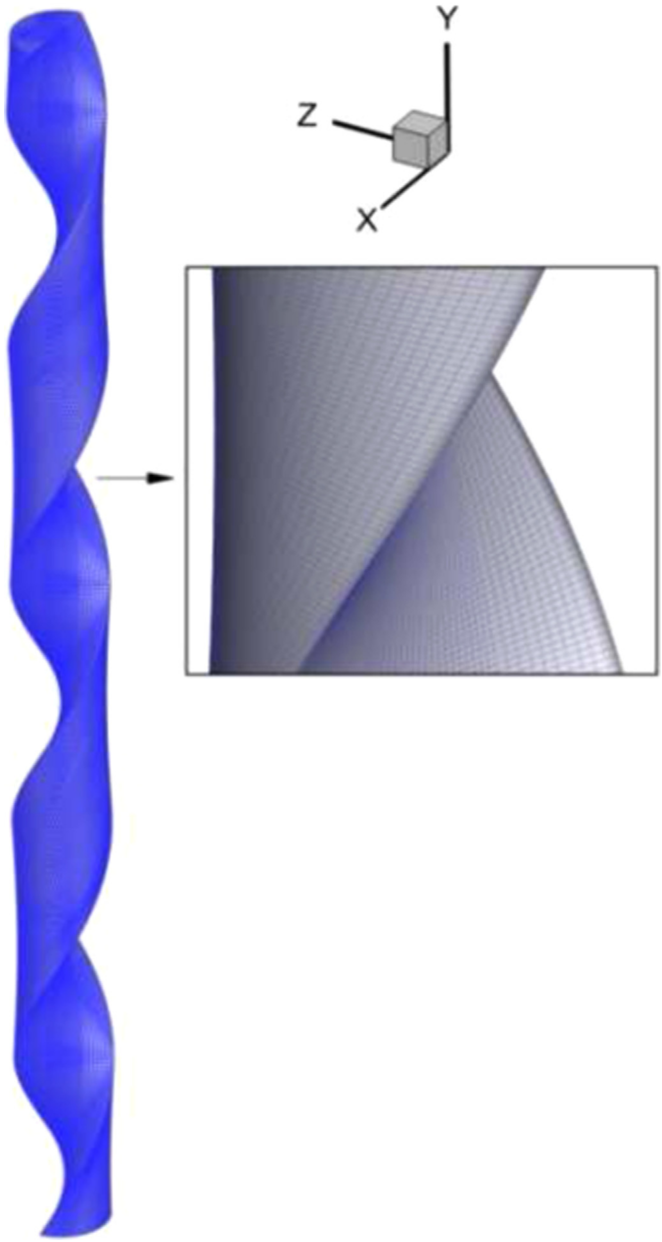

Fig. 2. Mesh of nozzle with twisted tape.

Table 1
Effect of mesh size on the Nusselt number.

Element size	0.4 mm	0.5 mm	0.6 mm	0.8 mm
Element volume/domain volume	1.28e-7	2.5e-7	4.3e-7	1.02e-6
Average Nusselt number	84.65	84.07	80.12	76.45

stagnation point and Reynolds Number near the stagnation zone (before striking), the surface average of Nusselt will be increased. Besides, the Nusselt number may have a local minimum at stagnation zone because of existence of twisted tape.

4.1. Effect of Reynolds number

As can be seen from Figs. 5 and 6, numerical results show that increasing the Reynolds number leads to an increase in the

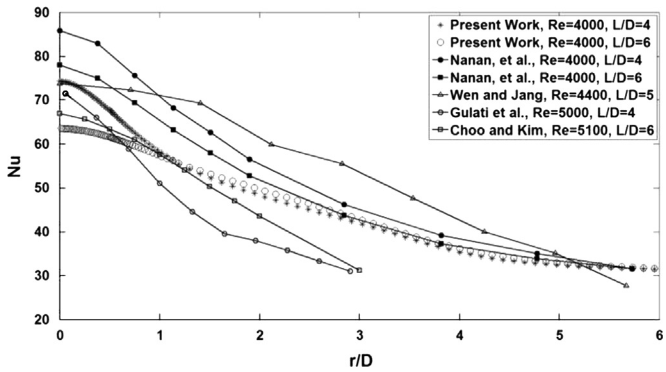

Fig. 3. Validation of numerical solution using the Nusselt number at impinging plate centerline.

Table 2
Various cases, which are studied in the present work.

Parameter	Values
Re	4000, 8000, 12,000, 16,000
L/*D*	2, 4, 6, 8
y/*w*	3, 4, 5, 6
Number of swirling jet	1, 2

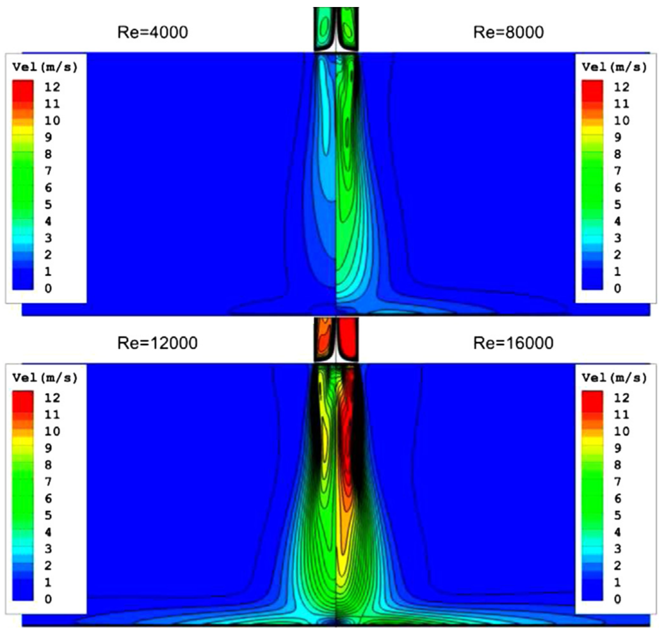

Fig. 4. Velocity contours under various Reynolds numbers ($L/D=6$, $y/w=3$).

heat transfer rate and, consequently, increases the Nusselt number. This is a general result, which holds four different jet-to-plate distances. For non-swirling jets, the straight striking of the jet to the impinged plate causes a high Maximum Nusselt number at the stagnation zone. Twisted tape can reduce the straight striking. Therefore, for the swirling jets the maximum local Nusselt number may be descended at the stagnation zone, besides, the presence of tape between two sides of stream ejected from one nozzle might reduce the velocity in the center of the jet and consequently reduce the Nusselt in Center of Stagnation zone, especially at low L/D ratios. Because in large L/D ratio, mixing and dispersing of two sides of the jet can reduce the effect of the existence of a gap between the streams. So as shown in Figs. 5 and 6, at $L/D=2$ and 4 a local minimum for Nusselt number exists.

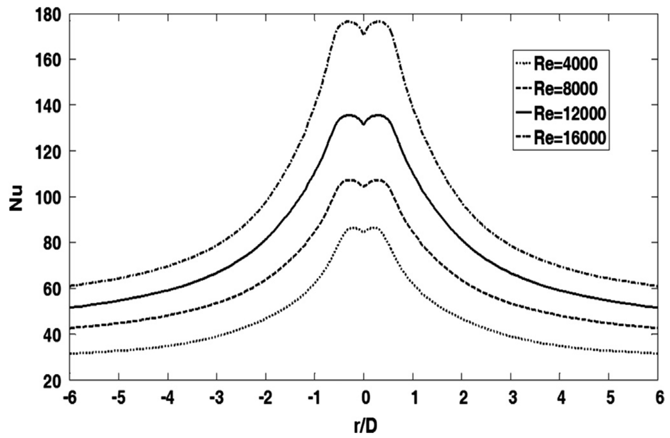

Fig. 5. Effect of Reynolds number on Nusselt ($L/D=2$, $y/w=3$).

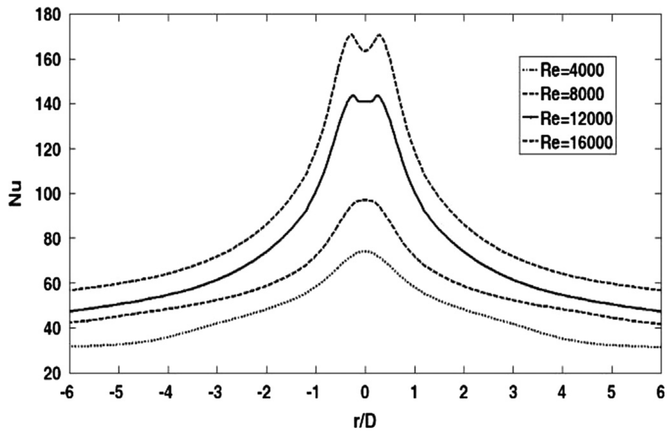

Fig. 6. Effect of Reynolds number on Nusselt ($L/D=4$, $y/w=3$).

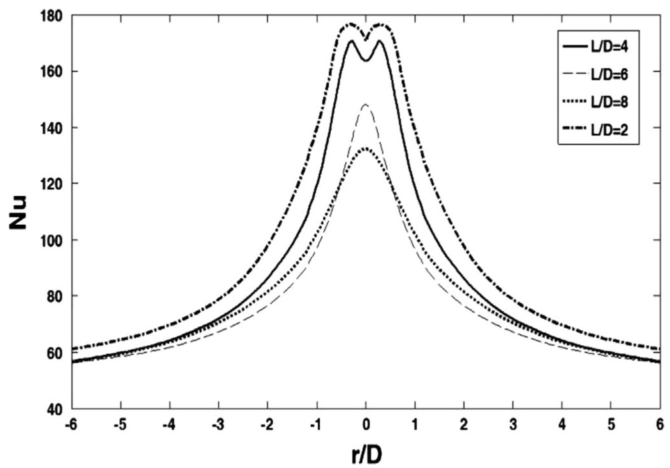

Fig. 7. Effect of L/D on Nusselt number (Re=16,000, $y/w=3$).

4.2. Effect of jet-to-plate distance

As can be observed in Fig. 7, in general, the low distance between the jet and the plate caused enhancing the heat

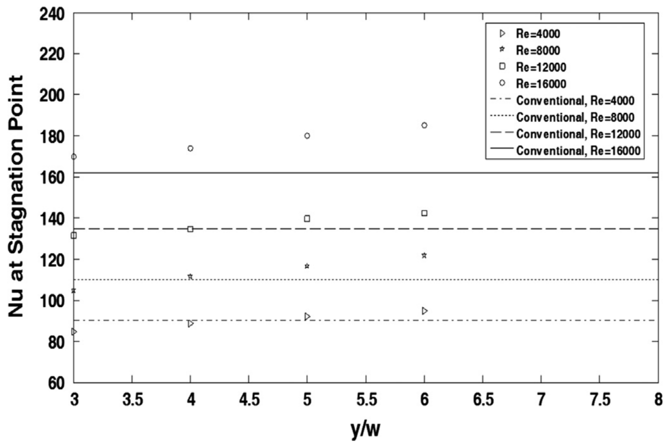

Fig. 8. Effect of twist tape ($y/w=3$) on Nusselt number of stagnation point ($L/D=2$).

transfer rate. This increase is more tangible at lower r/D ratios. It is noteworthy that the results experimentally gained by Nanan et al. [6], Choo et al. [28], Alekseenko et al. [29] and Wen and Jang [30] were the same as the present results.

Nonetheless, Fig. 7 reveals that, increasing L/D reduces the overall heat transfer rate. Although this is not desirable, the distribution of the local Nusselt number will be close to a uniform profile. This uniformity can be useful for specific purposes in which a uniform temperature profile is important.

4.3. Effect of twist ratio

To study the effect of the twist ratio on the Nusselt number at the stagnation point, computations for different cases were conducted. Jet impingements were considered for non-swirling and swirling cases under different Reynolds numbers and jet-to-plate distances. In Fig. 8, the Nusselt number at the stagnation point increases when the jet is swirled. The obtained results revealed the importance of swirling flow when high heat transfer rates are needed, especially at the stagnation zone. As shown in Fig. 8, in some cases using twisted tape may reduce the Nusselt number even to below of normal jet because the presence of tape between two sides of the stream might reduce the velocity in the center of the jet, especially at low $L/D=2$.

The Nusselt number at stagnation zone increases with increasing of twist ratio as revealed in Fig. 9. This increment is about 15% for $y/w=6$ in comparison with $y/w=3$ at region of $-1<r/D<1$.

The average Nusselt Number decreases with increasing of twist ratio because with increase in twist ratio (y/w) the swirling jet will be close to the normal jet.

4.4. Effect of using two jets

To study the effect of two jets on the Nusselt number in this investigation, several numerical solutions were done. The calculations were performed for $L/D=2$, 4, 6, and for four various Reynolds numbers from 4000 to 16,000.To compare these

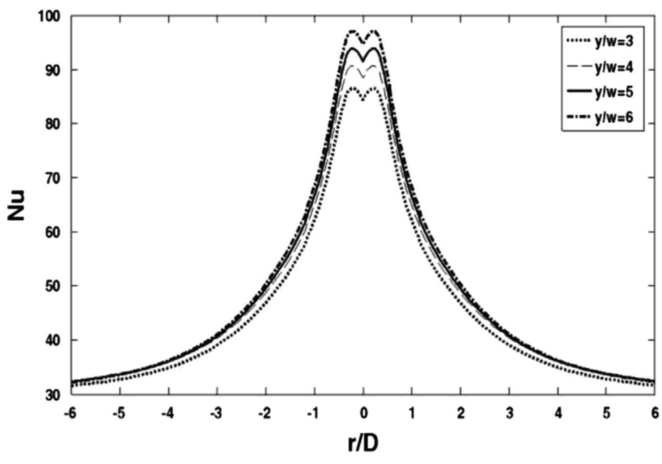

Fig. 9. Effect of twist ratio on Nusselt number (Re=4000, $L/D=2$).

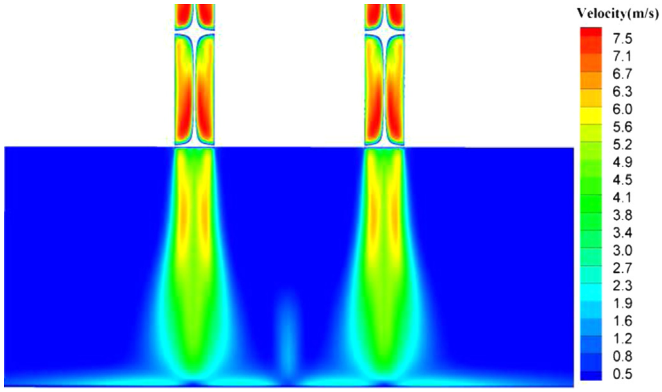

Fig. 10. Contour of velocity for two Nozzle (Re = 16,000, $L/D = 6$).

results with one-jet case, the Reynolds number was calculated based on the air flow rate and diameter of one jet, so the total amount of air flow ejected from two nozzle was equal to the one-jet case. However, the velocity of air in each nozzle was

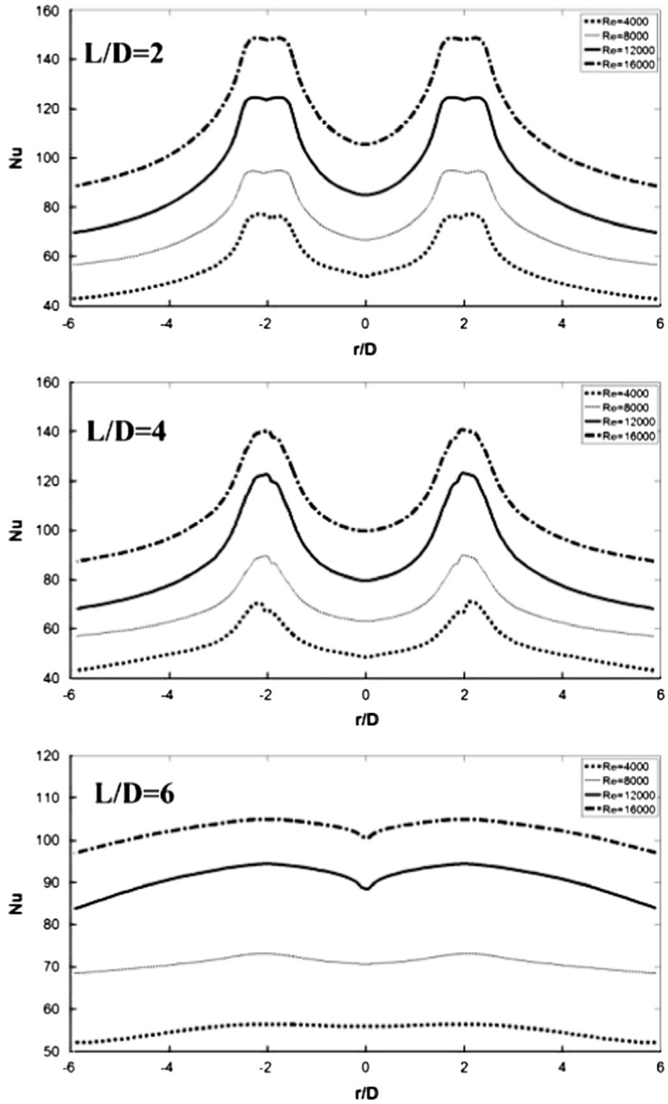

Fig. 11. Nusselt number of two-jet case.

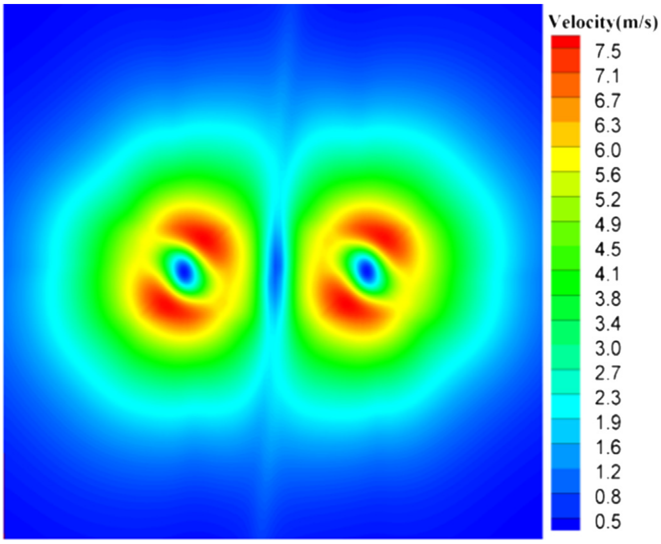

Fig. 12. Contour of velocity near the hot plate ($L/D=4$, Re=16,000).

half of the velocity of one-jet case. Fig. 10 shows the contour of velocity of air ejected from the nozzles.

With regard to the splitting of the air flow, it was predictable that the maximum Nusselt number of two-jet case should be less than of one-jet because of the reduction in velocity. In addition, it was expected that the overall Nusselt number increased due to the more uniformity of flow near the hot surface. The results justify this expectance.

Fig. 10 shows that the Nusselt number increases when the Reynolds number increases. Also for a high L/D, the Nusselt number profile approaches a linear profile due the mixing and dispersing of two jets.

At $r/D=0$ the Nusselt number has a local minimum point because of low air velocity, which this phenomenon is presented in Fig. 11. For small L/D ratio, decreasing in the Nusselt number at the stagnation point is occurred, because the air flow did not have a sufficient space, so the swirling flow regions could not be formed completely. Fig. 12 shows the air velocity on a face near the hot plate. It is obvious that at the stagnation point and at the point $r/D=0$ the air velocity reaches its minimum values.

For non-swirling jets, at the stagnation point, straight striking of jet to the hot plate causes the maximum Nusselt. Using twisted tape may remove the straight striking, so in the stagnation zone, the Nusselt may reduce, besides the existence of a gap between two sides of stream ejected from one nozzle as shown in Fig. 13, might reduce the velocity in center of the jet when L/D is low. Fig. 13 shows the velocity in the outlet section of the nozzle, which equipped with twisted tape. As obvious in Fig. 13, it is expected that in the center of the jet, which ejected from the nozzle, the velocity should be minimum.

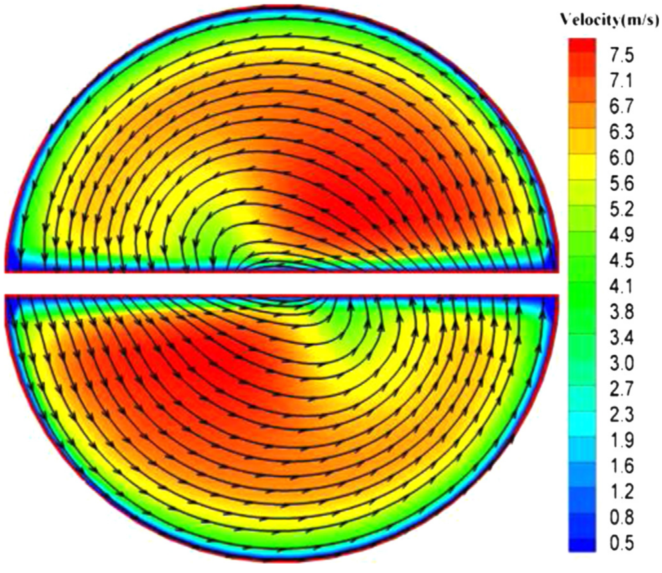

Fig. 13. Contour of velocity and stream line in one nozzle exhaust ($L/D=4$, Re=16,000).

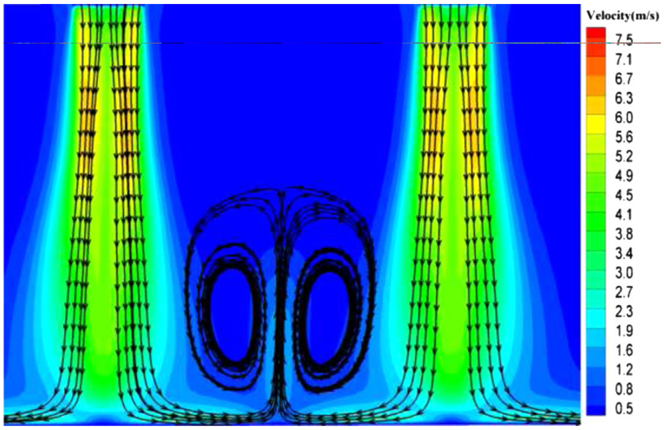

Fig. 14. Stream lines and contour of velocity (L/D=4, Re= 16,000).

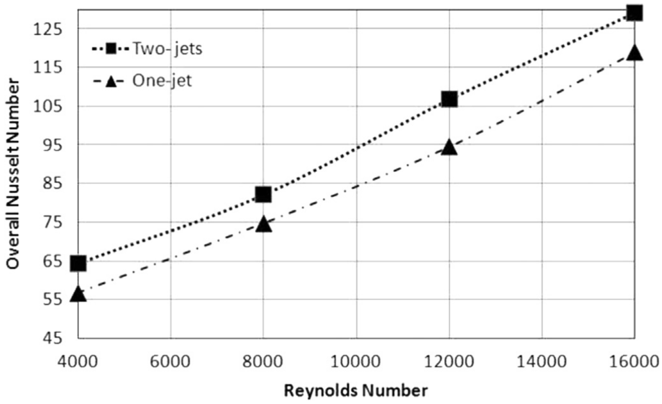

Fig. 15. Effect of using two jets (L/D=2).

Moreover, in the middle of the two jets, striking two streams gives rise to smaller amounts of velocity and Nusselt number. Fig. 14, presenting the streamlines of two jets, shows how these jets mixes, resulting in lower velocities.

To compare the heat transfer rate of the two-jet case with one-jet, the overall Nusselt number was computed and is shown in Fig. 15. The results show that the heat transfer rate is increased by using two nozzles instead of one because of better air circulation and The Nusselt number increased by approximately 10%, considering an equal air flow rate. In similar studies, Huang et al. [31] and Nuntadusit et al. [32] investigated the heat transfer rate of multiple non-swirling jets impinging on a plate, approving the present results. Accordingly, one can conclude that using multiple swirling jets can effectively increase the efficiency of the cooling process.

5. Conclusions

In the present research, the effects of the Nusselt number on the twist ratio (y/w), jet-to-plate distance (L/D), and the Reynolds number (Re) were numerically investigated. Simulations were conducted for twist ratios of 3, 4, 5 and 6, as well as jet-to-plate distances of 2, 4, 6 and 8 at different Reynolds numbers. The obtained results were validated through comparison with existing experimental results from the open literature. Simulation results showed that the best conditions for heat transfer were at jet-to-plate distances of 6 and 8, where the maximum Nusselt number occurred at the stagnation point (i.e., r/D=0) for the single jet. However, for L/D=2 and 4, the Nusselt number decreases at the stagnation point (as compared to the surrounding points) due to the effect of the twisted tape inserted in the nozzle jet. The other results were the greater influence of the Reynolds number on the Nusselt number as compared to the jet-to-plate distance and the twist ratio. Ultimately, the effect of using two nozzles was investigated with the results revealing that using two jets might give rise to higher heat transfer rates (enhancement of about 10%). Finally, the Nusselt number will approach a uniform profile if multiple nozzles with high jet-to-plate spacing are used.

References

[1] R.J. Goldstein, A.I. Behbahani, Impingement of a circular jet with and without cross flow, Int. J. Heat Mass Transf. 25 (1982) 1377–1382.
[2] M.B. Gerdroodbary, M. Imani, D.D. Ganji, Heat reduction using counterflowing jet for a nose cone with Aerodisk in hypersonic flow, Aerosp. Sci. Technol. 39 (2014) 652–665.
[3] M. Barzegar Gerdroodbary, Numerical analysis on cooling performance of counterflowing jets over aerodisked blunt body, Shock Waves 24 (2014) 537–543.
[4] A. Ianiro, G. Cardone, Heat transfer rate and uniformity in multichannel swirling impinging jets, Appl. Therm. Eng. 49 (2010) 89–98.
[5] S.K. Saha, Thermo hydraulics of turbulent flow through rectangular and square ducts with axial corrugation roughness and twisted-tapes with and without oblique teeth, Exp. Therm. Fluid Sci. 34 (2010) 744–752.
[6] K. Nanan, K. Wongcharee, C. Nuntadusit, S. Eiamsa-ard, Forced convective heat transfer by swirling impinging jets issuing from nozzles equipped with twisted tapes, Int. Commun. Heat Mass Trans. 39 (2012) 844–852.
[7] V. Katti, S.V. Prabhu, Experimental study and theoretical analysis of local heat transfer distribution between smooth flat surface and impinging air jet from a circular straight pipe nozzle, Int. J. Heat Mass Transf. 51 (2008) 4480–4495.
[8] M.J. Tummers, J. Jacobse, S.G.J. Voorbrood, Turbulent flow in the near field of a round impinging jet, Int. J. Heat Mass Transf. 55 (2011) 4939–4948.
[9] S. Eiamsa-ard, P. Promvonge, Enhancement of heat transfer in a tube with regularly-spaced helical tape swirl generators, Sol. Energy 78 (2005) 483–494.
[10] S. Eiamsa-ard, K. Wongcharee, S. Sripattanapipat, 3-D Numerical simulation of swirling flow and convective heat transfer in a circular tube induced by means of loose-fit twisted tapes, Int. Commun. Heat Mass Transf. 36 (2009) 947–955.
[11] S. Eiamsa-ard, C. Thianpong, P. Eiamsa-ard, P. Promvonge, Convective heat transfer in a circular tube with short-length twisted tape insert, Int. Commun. Heat Mass Trans. 36 (2009) 365–371.
[12] S. Ndao, H.J. Lee, Y. Peles, M.K. Jensen, Heat transfer enhancement from micro pin fins subjected to an impinging jet, Int. J. Heat Mass Transf. 55 (2012) 413–421.
[13] B. Sagot, G. Antonini, F. Buron, Enhancement of jet-to-wall heat transfer using axisymmetric grooved impinging plates, Int. J. Therm. Sci. 49 (2010) 1026–1030.
[14] M. Rahimi, S.R. Shabanian, A.A. Alsairafi, Experimental and CFD studies on heat transfer and friction factor characteristics of a tube equipped with modified twisted tape inserts, Chem. Eng. Process. 48 (2009) 762–770.
[15] K. Kanokjaruvijit, R.F. Martinez-Botas, Heat transfer correlations of perpendicularly impinging jet on a hemispherical-dimpled surface, Int. J. Heat Mass Trans. 53 (2012) 3045–3056.
[16] P. Gulati, V. Katti, S.V. Prabhu, Influence of the shape of the nozzle on local heat transfer distribution between smooth flat surface and impinging air jet, Int. J. Thermal Sci. 48 (2009) 602–617.
[17] S.D. Salman, Abdul Amir H. Kadhum, M.S. Takriff, A. Mohamad, Experimental and numerical investigations of heat transfer characteristics for impinging swirl flow, Adv. Mech. Eng. 2014 (2014) 1–9.
[18] M. Wannassi, F. Monnoyer, Fluid flow and convective heat transfer of combined swirling and straight impinging jet arrays, Appl. Therm. Eng. 78 (2015) 62–73.
[19] S. Caliskan, S. Baskaya, T. Calisir, Experimental and numerical investigation of geometry effects on multiple impinging air jets, Int. J. Heat Mass Transf. 75 (2014) 685–703.
[20] J.Y. San, J.J. Chen, Effects of jet-to-jet spacing and jet height on heat transfer characteristics of an impinging jet array, Int. J. Heat Mass Transf. 71 (2014) 817.
[21] K.M. Saqr, M.A. Wahid, Effects of swirl intensity on heat transfer and entropy generation in turbulent decaying swirl flow, Appl. Therm. Eng. 70 (2014) 486–493.
[22] M.B. Gerdroodbary, M. Rahimi, D.D. Ganji, Investigation of thermal radiation on traditional Jeffery-Hamel flow to stretchable convergent/divergent channels, Case Stud. Therm. Eng. 6 (2015) 28–39.
[23] M.B. Gerdroodbary, S.M. Hosseinalipour, Numerical simulation of hypersonic flow over highly blunted cones with spike, Acta Astronaut. 67 (1–2) (2010) 180–193.
[24] M.B. Gerdroodbary, Sh Bishehsari, S.M. Hosseinalipour, K. Sedighi, Transient analysis of counterflowing jet over highly blunt cone in hypersonic flow, Acta Astronaut. 73 (2012) 38–48.
[25] M.B. Gerdroodbary, M. Imani, D.D. Ganji, Investigation of film cooling on nose cone by a forward facing array of micro-jets in Hypersonic flow, Int. Commun. Heat Mass Transf. 64 (2015) 42–49.
[26] M.B. Gerdroodbary, D.D. Ganji, Y. Amini, Numerical study of shock wave interaction on transverse jets through multiport injector arrays in supersonic crossflow, Acta Astronaut. 115 (2015) 422–433.
[27] M. Barzegar Gerdroodbary, O. Jahanian, M. Mokhtari, Influence of the angle of incident shock wave on mixing of transverse hydrogen micro-jets in supersonic crossflow, Int. J. Hydrog. Energy 40 (2015) 9590–9601.
[28] K.S. Choo, S.J. Kim, Heat transfer characteristics of impinging air jets under a fixed pumping power condition, Int. J. Heat Mass Transf. 53 (2010) 320–326.
[29] S.V. Alekseenko, A.V. Bilsky, V.M. Dulin, D.M. Markovich, Experimental study of an impinging jet with different swirl rates, Int. J. Heat Fluid Flow 28 (2007) 1340–1359.
[30] M. Wen, K. Jang, An impingement cooling on a flat surface by using circular jet with longitudinal swirling strips, Int. J. Heat Mass Transf. 46 (2003) 4657–4667.
[31] L. Huang, M.S. EL-Genk, Heat transfer and flow visualization experiments of swirling, multi-channel, and conventional impinging jets, Int. J. Heat Mass Transf. 41 (1998) 583–600.
[32] C. Nuntadusit, M. Wae-hayee, A. Bunyajitradulya, S. Eiamsa-ard, Heat transfer enhancement by multiple swirling impinging jets with twisted-tape swirl generators, Int. Commun. Heat Mass Transf. 39 (2011) 102–107.